

Constraining strongly supercooled phase transitions by overproduction of black holes

Marek Lewicki^{1,2,*} and Ville Vaskonen^{1,3,†}

¹*Physics Department, King's College London, London WC2R 2LS, UK*

²*Faculty of Physics, University of Warsaw ul. Pasteura 5, 02-093 Warsaw, Poland*

³*NICPB, R vala 10, 10143 Tallinn, Estonia*

We study the formation of black holes from bubble collisions in cosmological first order phase transitions. We show that if false vacuum bubbles are formed in these collisions, new very strong constraints can be put on models due to overproduction of black holes.

Recently there has been considerable interest in formation of black holes (BHs) in the early universe. The studies have focused, in the spirit of Refs. [1, 2], on the formation from large density contrasts formed during inflation. Meanwhile alternative formation scenarios have received surprisingly little attention. These include for example formation of BHs from overdensities generated in a first order phase transition [3–5].

A first order phase transition proceeds by nucleation of bubbles of the new vacuum state. These bubbles then expand, collide and finally turn the whole universe in the true vacuum state. It is possible that the vacuum energy of the false vacuum surpasses the thermal energy before the transition finishes. In this case the bubble walls accelerate almost to the speed of light and accumulate a large amount of energy.

The first attempts to form BHs in this kind of strongly supercooled phase transition focused on trying to use the overdensities caused by multiple bubble walls intersecting at one point [3]. However, the volumes containing enough energy for gravitational collapse are much larger than the intersection point and the system is then very far from being spherically symmetric [6]. Therefore, the BH formation via this mechanism is not likely.

Another proposed mechanism relies on gravitational collapse of small regions of false existing still just before the transition completes [4]. However, such final false vacuum regions left between growing bubbles are not spherically symmetric. In fact the energy contained in such a region drops quickly as it shrinks. For this reason a dedicated numerical study is necessary to verify their collapse and possible density of BHs that could potentially be produced. We will not discuss this mechanism further.

Finally, in collision of very energetic bubble walls it is possible that the scalar field bounces to a false vacuum phase. A false vacuum bubble (FVB) is formed that eventually becomes spherical, starts to shrink and can collapse to a BH. This mechanism of BH formation was introduced in Ref. [5]. In this paper we refine their analysis in order to be able to draw phenomenological conclusions. This mechanism proves to be much more promising and, together with recent developments concerning dynamics of energetic wall collisions [7], allows us to put new very stringent constraints on particle physics

models predicting a strongly supercooled phase transition.

Throughout this paper we use natural units where $c = \hbar = 1$. The physical bubble radius R at time t , assuming that bubbles grow with constant velocity $v_w \approx 1$ and neglecting their small initial size, is

$$R(\tilde{t}, t) = a(t) \int_{\tilde{t}}^t \frac{dt'}{a(t')}, \quad (1)$$

where $\tilde{t} < t$ is the time when the bubble was formed. Assuming that the transition happens during vacuum dominance, $H = \text{constant}$, $a(t) \propto e^{Ht}$, the radius is given by

$$R(\tilde{t}, t) = H^{-1} \left(e^{H(t-\tilde{t})} - 1 \right). \quad (2)$$

The bubbles that will engulf a given point at time t since the nucleation begun at t_c are all nucleated within a sphere of radius $R(t_c, t)$. Thus, the expected number of bubbles, without taking into account overlaps, at a given point is [8, 9]

$$N_b(t) = \frac{4\pi}{3} \int_{t_c}^t d\tilde{t} a(\tilde{t})^3 \Gamma(\tilde{t}) \left(\frac{R(\tilde{t}, t)}{a(t)} \right)^3, \quad (3)$$

where $\Gamma(t)$ is the nucleation rate of bubbles in unit volume and time. Since this is a Poisson distributed variable, the probability that no bubble has converted a given point to the true vacuum is simply

$$P_F(t) = e^{-N_b(t)}, \quad (4)$$

and the number density of bubbles nucleated within time interval $(t, t + dt)$ is

$$dn_n(t) = P_F(t) \Gamma(t) dt. \quad (5)$$

Let us consider two bubbles nucleated at times t_1 and $t_2 \geq t_1$ at distance $d > t_2 - t_1 = \Delta t$ from each other, as shown in Fig. 1. Approximating that both bubbles grow with $v_w \approx 1$, their walls collide at $t = (d + \Delta t)/2 + t_1$. Assume now that an expanding region where the system is in the false vacuum is formed around the collision point. The expansion of this FVB stops when all of the kinetic energy of the walls is converted into potential energy. The FVB then starts to shrink and eventually bounces

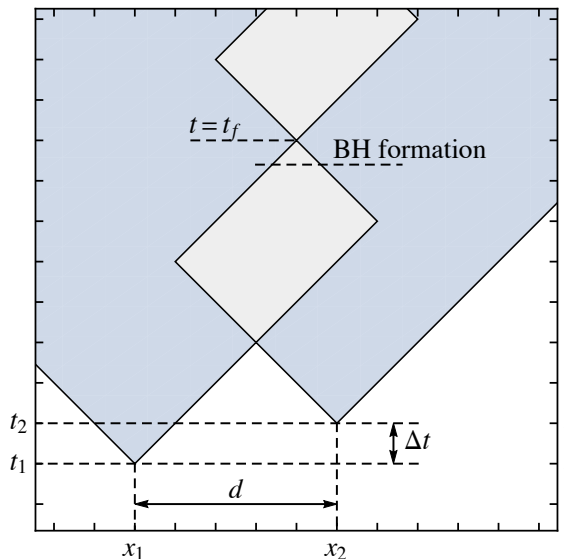


FIG. 1. A schematic plot of collision of two bubbles. The white region corresponds to initial false vacuum phase. Inside the bubbles is the true vacuum phase (blue) and in their collision a false vacuum bubble (gray) is formed.

again, unless it collapses into a BH before that. The FVB can not collapse at the early stages of the expanding phase because it is not spherical, but the surface tension of the wall makes the FVB spherical so that the gravitational collapse is possible near the end of the shrinking phase.

Neglecting friction and the initial bubble sizes, the maximum volume of the FVB formed in the collision is given by

$$V_f(\Delta t, d) = \frac{\pi R_2^3(8R_1 - 3R_2)}{12 R_1}, \quad (6)$$

where $R_1 = d$ and $R_2 = d - \Delta t$ are the radii of the bubbles when that volume is reached. The mass of the

FVB is then

$$M(\Delta t, d) = V_f(\Delta t, d)\Delta V, \quad (7)$$

where $\Delta V = \zeta \times 3H^2/(8\pi G)$ is the potential energy difference between the true and false vacuum bubbles. We introduced the parameter $\zeta > 0$, as the vacuum energy density inside the FVB is not necessarily equal to the vacuum energy density that dominates the expansion rate. As the FVB shrinks it does not lose mass and it will collapse into a BH if the minimum radius of the FVB, given by the wall width l of the FVB, is smaller than the Schwarzschild radius of the mass M ,

$$l < 2MG. \quad (8)$$

Roughly, the abundance of BHs can be estimated as follows: If the average bubble radius at the time of their collisions is $R_* = \epsilon H^{-1}$, then the Hubble horizon includes $\mathcal{O}(1/\epsilon^3)$ bubbles and therefore the collisions have produced $N \sim 1/\epsilon^3$ BHs. The mass of these BHs is $M \sim R_*^3 \rho \sim \epsilon^3 M_H$, where M_H is the total mass of the Hubble patch. This oversimplified reasoning would suggest that these BHs make up a fraction $NM/M_H \sim 1$ of the total energy density. However, for a more accurate estimate we need to avoid overlaps between FVBs which would lead to doublecounting.

The number density of the configurations shown in Fig. 1 is

$$dn_c(t_1, t_2, d) = 4\pi d^2 P_F(t_f) dn_n(t_1) dn_n(t_2) dd, \quad (9)$$

where $t_f = (3d + \Delta t)/2 + t_1$ is the time when the FVB bounces again if it has not collapsed gravitationally. The factor $P_F(t_f)$ ensures that no other bubble walls have intersected the FVB, and therefore avoids the doublecounting. From this, we can calculate the number density of BHs at time t with mass in the range $(M, M + dM)$ formed from those configurations,

$$\begin{aligned} dn_{\text{BH}}(M, t) &= dM \int dn_c(t_1, t_2, d) \left(\frac{a(t_f)}{a(t)} \right)^3 \delta(M - M(\Delta t, d)) \theta(2MG - l) \\ &= 4\pi dM \int dt_1 dt_2 \left(\frac{a(t_f)}{a(t)} \right)^3 P_F(t_f) P_F(t_1) P_F(t_2) \Gamma(t_1) \Gamma(t_2) \theta(2MG - l) d^2 \left| \frac{dM(\Delta t, d)}{dd} \right|^{-1} \Big|_{d=d(\Delta t, M)}. \end{aligned} \quad (10)$$

This estimate neglects the Hawking evaporation of the formed BHs, which we will take into account later. The expansion rate of the universe changes when the transition finishes (unless the abundance of BHs becomes dominant before that). This happens roughly at the percolation time $t = t_p$ defined via $N_b(t_p) = 0.34$.

Let us now consider the following approximation for

the bubble nucleation rate,

$$\Gamma(t) = H^4 e^{\beta(t-t_n)}, \quad (11)$$

where $\beta > 0$ is the inverse time scale of the transition, and t_n is the bubble nucleation time, defined, as usual, via $\Gamma(t_n) = H^4$. Moreover, let us assume that a FVB with $\zeta = 1$ is formed in every collision and that the con-

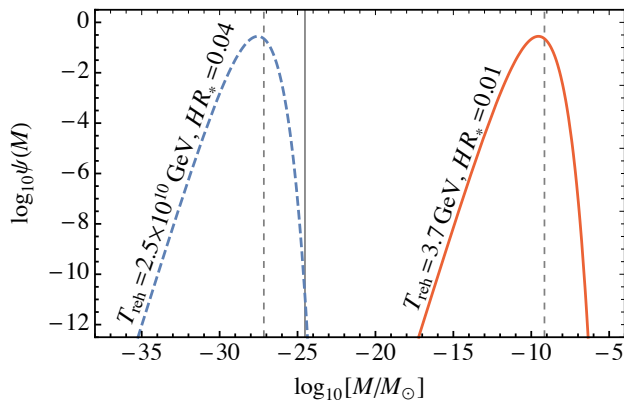


FIG. 2. Two examples of the BH mass function formed in a phase transition from collapsing FVBs. The solid vertical line indicates the highest mass BHs that evaporate before big-bang nucleosynthesis. The dashed vertical lines indicate the mean masses of the distributions.

dition (8) is always satisfied, i.e. all of the FVBs collapse to BHs. We will discuss these assumptions in a toy model later.

We now have only two free parameters: H and β .¹ The Hubble rate we can trade for the temperature of the plasma after the vacuum energy has decayed, T_{reh} through the relation $\rho_\gamma(T_{\text{reh}}) = 3H^2/(8\pi G)$, and β we trade for the average bubble radius at percolation,

$$R_* = (8\pi)^{1/3} \beta^{-1}, \quad (12)$$

which is a fraction of the Hubble radius H^{-1} .

Two examples of the produced normalized mass function,

$$\psi(M) = \frac{M}{n_{\text{tot}}} \frac{dn_{\text{BH}}(M)}{dM}, \quad (13)$$

where $n_{\text{tot}} = \int dn_{\text{BH}}(M)$ is the total number density of BHs, are shown in Fig. 2. The shape of the mass function around the peak is well approximated by

$$\psi(M) \propto M^2 \exp \left[-10(M/\langle M \rangle)^{1/4} \right]. \quad (14)$$

The dashed vertical lines show the mean masses of the spectra

$$\langle M \rangle / M_\odot \approx M(0, R_*) / 2 = 10^{-20} (HR_*)^3 \text{ GeV} / H. \quad (15)$$

The total energy density of BHs,

$$\rho_{\text{BH}} = \int dn_{\text{BH}}(M) M, \quad (16)$$

as a fraction of the total energy density ρ_{tot} of the universe at $t = t_p$ is shown as a function of HR_* in Fig. 3.

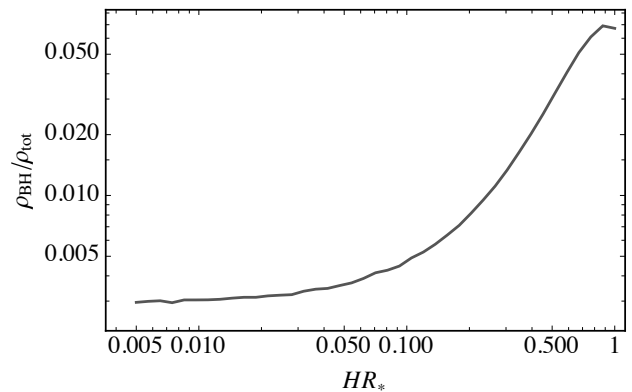


FIG. 3. The fraction of the total energy density of the universe at the percolation time in BHs formed in bubble collisions as a function of the average bubble radius at percolation in Hubble radii.

The abundance does not change significantly for different values of H (or T_{reh}) and decreases together with HR_* reaching asymptotically a constant value of $\sim 0.3\%$.

So abundant BHs quickly start to dominate the energy density of the universe after their formation. The only way to reconcile this result with existing bounds is for the BHs to evaporate via Hawking radiation [10, 11] before big-bang nucleosynthesis [12]. BHs of mass less than $10^{-24} M_\odot$ evaporate in time

$$\tau_{\text{evap}} \simeq 3 \text{ s} \left(\frac{M}{10^{-24} M_\odot} \right)^3. \quad (17)$$

When they evaporate they produce all particles reheating the radiation bath.² The temperature when BHs of mass M evaporate is

$$T_{\text{evap}} \simeq \frac{8 \times 10^{-4}}{g_*(T_{\text{evap}})^{1/4}} \left(\frac{M}{10^{-24} M_\odot} \right)^{-3/2}, \quad (18)$$

where $g_*(T)$ denotes the effective number of relativistic degrees of freedom. This is smaller than the temperature when they start to dominate over the radiation energy density, if

$$\frac{M}{10^{-24} M_\odot} \gtrsim 0.04 g_*(T_{\text{reh}})^{-2/9} T_{\text{reh}}^{-2/3}. \quad (19)$$

Using Eq. (15) we get that the BHs become the dominant energy density component before they evaporate if

$$HR_* \gtrsim 10^{-8} g_*(T_{\text{reh}})^{5/54} T_{\text{reh}}^{4/9}. \quad (20)$$

This is shown by the yellow solid line in Fig. 4.

¹ Without loss of generality, we can take $t_n = 0$.

² This may also give raise for example to the observed dark matter abundance [13–15].

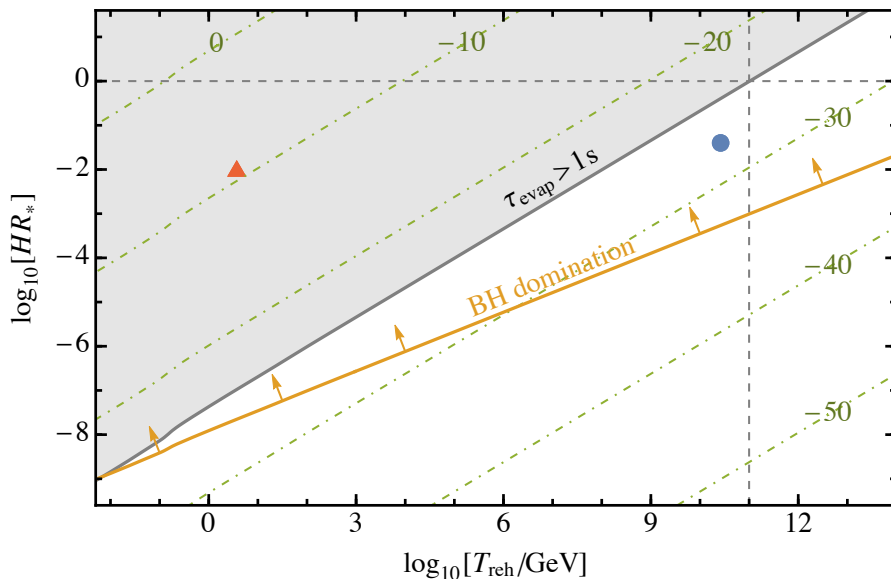


FIG. 4. The shaded gray region is excluded by overproduction of BHs that do not evaporate before big-bang nucleosynthesis. Above the yellow solid line the BHs dominate the energy density of the universe before they evaporate. The labelled dot-dashed lines show the peak mass of the BH mass function, $\log_{10}((M)/M_{\odot})$. The blue circle and the red triangle correspond to the example cases shown in Fig. 2 with the same colours. The left boundary of the plot corresponds to $T_{\text{reh}} = 5$ MeV.

For a successful big-bang nucleosynthesis these BHs have to evaporate in less than one second. Using Eq. (15) and requiring that $M \lesssim 7 \times 10^{-25} M_{\odot}$, in which case $\tau_{\text{evap}} < 1$ s, gives a bound

$$HR_* \lesssim 3 \times 10^{-8} g_*(T_{\text{reh}})^{1/6} T_{\text{reh}}^{2/3}, \quad (21)$$

shown in Fig. 4. For $T_{\text{reh}} \gtrsim 10^{11}$ GeV the upper bound is not relevant as R_* can not be larger than the Hubble radius. This corresponds to the region right from the dashed vertical line. The cases shown in Fig. 2 are indicated by the blue point and the red triangle.

Let us next illustrate our results in a simple toy model described at finite temperature by a potential

$$V(\varphi, T) = \frac{m^2 + g^2 T^2}{2} \varphi^2 - \frac{\kappa}{3} \varphi^3 - \frac{\kappa'}{3} |\varphi|^3 + \frac{\lambda}{4} \varphi^4, \quad (22)$$

where $g, \kappa, \kappa', \lambda > 0$. At $T > -m/g$ this potential has a minimum at $\varphi = 0$, which at $T > T_c$,

$$T_c^2 = \frac{2}{9g^2\lambda} (\kappa + \kappa')^2 - \frac{m^2}{g^2}, \quad (23)$$

is the global minimum of the potential. Eventually a minimum at $\varphi > 0$ develops and becomes the global minimum. The bubble nucleation rate per unit time and volume is given by [16–18]

$$\Gamma(T) \simeq T^4 \left(\frac{S_3}{2\pi T} \right)^{\frac{3}{2}} \exp\left(-\frac{S_3}{T}\right), \quad (24)$$

	m^2	g	κ	κ'	λ
red	10^8	1	10^7	7×10^5	10^{-6}
blue	10^{-11}	0.004	9×10^{-6}	5×10^{-7}	10^{-9}

TABLE I. Values for the parameters used in the examples for our toy-model potential.

where

$$S_3 = 4\pi \int r^2 dr \left[\frac{1}{2} \left(\frac{d\varphi}{dr} \right)^2 + V(\varphi, T) \right] \quad (25)$$

is the action for an O(3)-symmetric bubble corresponding to the path that extremizes S_3 .

To approximate S_3 , we use the fit given in Ref. [19]. The nucleation rate can be approximated by (11) with β given by

$$\beta = HT \frac{d}{dT} \frac{S_3}{T}. \quad (26)$$

To check whether a given point of the parameter space of a model is at odds due to BH overproduction we have to: 1) check if transition occurs during vacuum domination, 2) if produced FVBs collapse into BHs, and 3) the field gets trapped in the false vacuum in bubble collisions. We do this explicitly for two example sets of parameters indicated in Table I.

First, both our examples predict very strong transitions with $\rho_V/\rho_R > 10^7$ and our earlier assumption of vacuum dominated expansion can be safely used. In fact

such strongly supercooled transitions are necessary if a significant amount of energy is to be stored within the bubble walls. Even though the specific strength required for this to be realised depends on the particle content and their couplings we will assume that this is true in our examples (see [20] for more general treatment).

Second, let us consider the assumption that if a FVB is formed, it will with certainty collapse to a BH. Very conservatively we can assume that the bubble wall width at the moment when the BH is formed if the condition (8) is satisfied is $l < 2R_0$. The inequality $2R_0 < 2MG$ then ensures that the condition (8) is safely satisfied. The initial radii of the bubbles in our examples are $HR_0 = 10^{-18}$ (red) and $HR_0 = 2 \times 10^{-9}$ (blue) and the above bound gives $M > 10^{-20}M_\odot$ (red) and $M > 10^{-30}$ (blue). These lower bounds are well below the mean masses of the formed BH distributions.

Third assumption that we need to address concerns the formation of the FVBs in the transition predicted by our toy model. We will use the method described in [7] (see also [21–23]) which involves solving the trapping equation

$$\frac{d^2\varphi}{dt^2} + \frac{1}{t} \frac{d\varphi}{dt} = -\frac{dV}{d\varphi} \quad (27)$$

that describes a collision of two identical bubbles. We already fixed the spatial position to describe the time evolution of the field in the collision point and verify whether a FVB is formed. At the moment of collision the two field profiles simply add so for each potential we need to solve (27) with the initial value for the field equal to twice its vacuum expectation value, $\varphi(t=0) = 2\phi_{\min}$.

We illustrate trapping with our two example sets of parameters in Fig 5. The corresponding potentials are shown in the upper panel and the evolution of the field at collision point of two bubbles in the lower panel. In both cases the transition begins as the field tunnels from the very shallow local minimum at $\phi = 0$ to the global one at $\phi > 0$. However, after a collision of bubbles the field is trapped in the false vacuum at $\phi < 0$ forming FVBs that will disappear as the transition finishes. In this case the parameter ζ that we introduced below Eq. (7) is $\zeta \sim 0.5$, introducing a 0.5 factor for the masses of the BHs compared to what is shown in Figs. 2 and 4. Neglecting that small modification, our example sets correspond to the results shown in Figs. 2 and 4 by the same colours as in Fig. 5.

As we see in Fig. 4 the vastly different values of parameters in both our points result in a huge difference of reheating temperatures. However, the typical size of the bubbles in Hubble radii, HR_* , is quite similar. This is a rather generic result because as already mentioned we need significant supercooling to overcome friction from the plasma to deposit energy into the field profiles. Such supercooled solutions typically have very large ρ_V/ρ_R and rather large $HR_* \gtrsim 10^{-2}$ [20]. Taking this into account we can generally say that overproduction of BHs

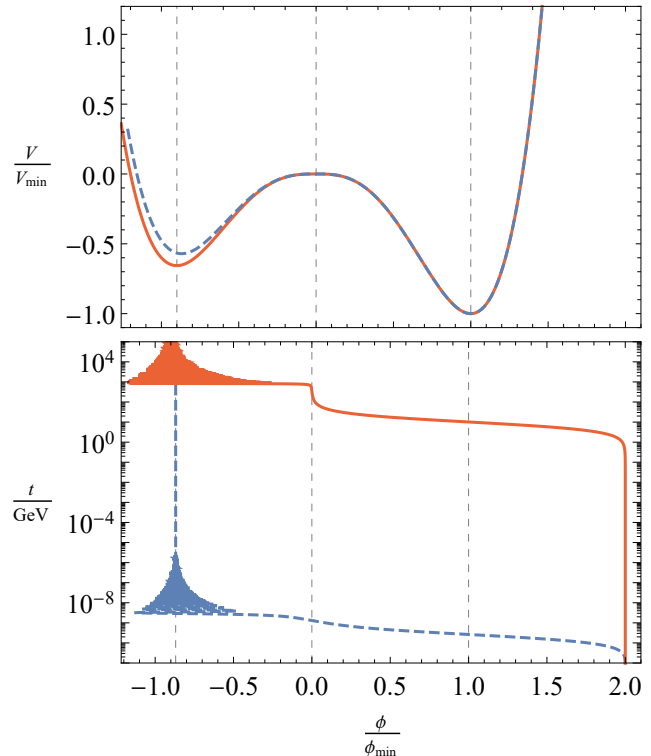


FIG. 5. Upper panel: Examples of a potential (22) realising a very strong transition. Lower panel: evolution of the field at the point of collision of two identical bubbles. These examples correspond to the cases shown in Figs. 2 and 4 indicated by the same colours.

will place very stringent constraints on models featuring a strongly supercooled phase transition. Essentially this rules out all models in which the temperature after the transition is $T_{\text{reh}} \lesssim 10^8$ GeV. Such high scale of reheating would necessarily push the corresponding gravitational wave (GW) signal sourced by the transition to frequencies too high for observation in any of the current or planned GW experiments.

The constraint that we obtained is only reliant on false vacuum trapping. This has two crucial consequences: 1) Observation of a GW signal consistent with production through bubble collisions in a first order phase transition would point to models with potentials where false vacuum trapping is not possible. 2) Analysis of models generically featuring a strong phase transition should necessarily be accompanied by analysis of false vacuum trapping to make sure the model is not already ruled out. The second point is especially important for models featuring a new strongly interacting sector not far above the TeV scale [24–27]. Such models generically predict a strong transition and could be excluded due to this bound. The main difficulty there comes from scrutiniz-

ing the dynamics of the transition to ascertain whether false vacuum trapping occurs. Going back to the first point, we checked that certain models can be safe from this constraint. We made sure that false vacuum trapping does not occur in classically conformal $U(1)_{B-L}$ model (see [20, 28] for details) despite a strong phase transition producing a GW signal through collisions of bubbles.

While all arguments seem to point to a gravitational collapse of the FVB in to a BH a direct numerical proof would be desirable. On that same note a numerical verification of the lack of collapse on intersection of multiple walls and non-spherically symmetric false vacuum remnants would be just as useful. However, this further confirmation of the robustness of our bounds is beyond the scope of this work and for the moment we leave it as a possible avenue for future work.

Acknowledgments: We thank Miguel Escudero, Kimmo Kainulainen and Eugene Lim for discussions. We would also like to express our gratitude to Nordita and CERN Theory Division who hosted us during our work on this project. This work was supported by the UK STFC Grant ST/P000258/1. ML was partly supported by the Polish National Science Center grant 2018/31/D/ST2/02048.

* marek.lewicki@kcl.ac.uk

† ville.vaskonen@kcl.ac.uk

- [1] B. J. Carr and S. W. Hawking, Mon. Not. Roy. Astron. Soc. **168**, 399 (1974).
- [2] B. J. Carr, Astrophys. J. **201**, 1 (1975).
- [3] S. W. Hawking, I. G. Moss, and J. M. Stewart, Phys. Rev. **D26**, 2681 (1982).
- [4] H. Kodama, M. Sasaki, and K. Sato, Prog. Theor. Phys. **68**, 1979 (1982).
- [5] M. Yu. Khlopov, R. V. Konoplich, S. G. Rubin, and A. S. Sakharov, (1998), arXiv:hep-ph/9807343 [hep-ph].
- [6] I. G. Moss, Phys. Rev. **D50**, 676 (1994).
- [7] R. Jinno, T. Konstandin, and M. Takimoto, JCAP **1909**, 035 (2019), arXiv:1906.02588 [hep-ph].
- [8] A. H. Guth and S. H. H. Tye, Phys. Rev. Lett. **44**, 631 (1980), [Erratum: Phys. Rev. Lett.44,963(1980)].
- [9] A. H. Guth and E. J. Weinberg, Phys. Rev. **D23**, 876 (1981).
- [10] S. W. Hawking, Nature **248**, 30 (1974).
- [11] S. W. Hawking, Commun. Math. Phys. **43**, 199 (1975), [167(1975)].
- [12] B. J. Carr, K. Kohri, Y. Sendouda, and J. Yokoyama, Phys. Rev. **D81**, 104019 (2010), arXiv:0912.5297 [astro-ph.CO].
- [13] O. Lennon, J. March-Russell, R. Petrossian-Byrne, and H. Tillim, JCAP **1804**, 009 (2018), arXiv:1712.07664 [hep-ph].
- [14] L. Morrison, S. Profumo, and Y. Yu, JCAP **1905**, 005 (2019), arXiv:1812.10606 [astro-ph.CO].
- [15] D. Hooper, G. Krnjaic, and S. D. McDermott, JHEP **08**, 001 (2019), arXiv:1905.01301 [hep-ph].
- [16] S. R. Coleman, Phys. Rev. **D15**, 2929 (1977), [Erratum: Phys. Rev.D16,1248(1977)].
- [17] C. G. Callan, Jr. and S. R. Coleman, Phys. Rev. **D16**, 1762 (1977).
- [18] A. D. Linde, Nucl. Phys. **B216**, 421 (1983), [Erratum: Nucl. Phys.B223,544(1983)].
- [19] F. C. Adams, Phys. Rev. **D48**, 2800 (1993), arXiv:hep-ph/9302321 [hep-ph].
- [20] J. Ellis, M. Lewicki, J. M. No, and V. Vaskonen, JCAP **1906**, 024 (2019), arXiv:1903.09642 [hep-ph].
- [21] J. T. Giblin, Jr, L. Hui, E. A. Lim, and I.-S. Yang, Phys. Rev. **D82**, 045019 (2010), arXiv:1005.3493 [hep-th].
- [22] M. A. Amin, E. A. Lim, and I.-S. Yang, Phys. Rev. Lett. **111**, 224101 (2013), arXiv:1308.0605 [hep-th].
- [23] M. A. Amin, E. A. Lim, and I.-S. Yang, Phys. Rev. **D88**, 105024 (2013), arXiv:1308.0606 [hep-th].
- [24] P. Baratella, A. Pomarol, and F. Rompineve, JHEP **03**, 100 (2019), arXiv:1812.06996 [hep-ph].
- [25] S. Bruggisser, B. Von Harling, O. Matsedonskyi, and G. Servant, JHEP **12**, 099 (2018), arXiv:1804.07314 [hep-ph].
- [26] T. Konstandin and G. Servant, JCAP **1112**, 009 (2011), arXiv:1104.4791 [hep-ph].
- [27] L. Randall and G. Servant, JHEP **05**, 054 (2007), arXiv:hep-ph/0607158 [hep-ph].
- [28] C. Marzo, L. Marzola, and V. Vaskonen, Eur. Phys. J. **C79**, 601 (2019), arXiv:1811.11169 [hep-ph].